Drosophila p38 MAPK Interacts with BAG-3/starvin to Regulate Age-dependent Protein Homeostasis

Sarah M. Ryan[2,*], Michael Almassey[1,*], Amelia M. Burch[3], Gia Ngo[2], Scott Barbee[2], Nathan T. Mortimer[1], Subhabrata Sanyal[3,4] and Alysia D. Vrailas-Mortimer[1-3]

1 Illinois State University, School of Biological Sciences, Normal, IL, USA

2 University of Denver, Department of Biological Sciences, Denver, CO, USA

3 Emory University, Department of Cell Biology, Atlanta, GA, USA

4 Calico, San Francisco, CA, USA

Running Title: p38K Regulates Age-Dependent Proteostasis

Key words/phrases: p38 MAPK, BAG-3/starvin, protein aggregation, aging, Lamin

Corresponding author:
Alysia D. Vrailas-Mortimer
Illinois State University
School of Biological Sciences
Science Laboratory Building
Normal, IL 61790
Phone: 309-348-8574
Fax: 309-348-3722
e-mail: admorti@ilstu.edu

Summary

As organisms age, they often accumulate protein aggregates that are thought to be toxic, potentially leading to age-related diseases. This accumulation of protein aggregates is partially attributed to a failure to maintain protein homeostasis. A variety of genetic factors have been linked to longevity, but how these factors also contribute to protein homeostasis is not completely understood. In order to understand the relationship between aging and protein aggregation, we tested how a gene that regulates lifespan and age-dependent locomotor behaviors, p38 MAPK (p38Kb), influences protein homeostasis as an organism ages. We find that p38Kb regulates age-dependent protein aggregation through an interaction with the Chaperone-Assisted Selective Autophagy complex. Furthermore, we have identified Lamin as an age-dependent target of p38Kb and the Chaperone-Assisted Selective Autophagy complex.

Introduction

Protein turnover is critical for maintaining tissue health as many proteins become damaged or misfolded during normal tissue functions. Therefore, the cell utilizes a variety of protein quality control mechanisms to refold or degrade these damaged proteins, including the ubiquitin proteasome system and macroautophagy. During aging, protein quality control mechanisms become less efficient leading to the accumulation of damaged or misfolded proteins that begin to form protein aggregates[1]. It has been hypothesized that these aggregates are toxic and may lead to the deleterious phenotypes associated with normal aging, such as impaired tissue function[1]. Furthermore, decreased protein aggregation has been associated with longevity. For example, over-expression of Foxo leads to an increased lifespan but also a concordant

79 decrease in protein aggregation in *C. elegans*, *Drosophila,* and mice [2–6], suggesting that
80 lifespan and protein aggregation are tightly linked processes. However, the molecular
81 mechanisms that underlie the relationship between aging and protein homeostasis have
82 not been fully characterized.
83
84 One pathway that has been linked to both aging and protein homeostasis is the
85 stress response p38 MAPK (p38K) pathway. In mammals, there are four p38K genes (α,
86 β, γ, and δ), and p38Kα has been linked to both the inhibition [7,8] and induction [9,10] of
87 macroautophagy, in particular in response to oxidative stress [11,12]. In addition, p38Kα
88 has been linked to regulating macroautophagy in cellular senescence [13–15]. However,
89 how p38K signaling may contribute to protein homeostasis in response to natural aging
90 is not well understood. The fruit fly *Drosophila melanogaster* has two canonical p38K
91 genes (p38Ka and p38Kb), and we have previously reported that p38Kb acts in the adult
92 musculature to regulate aging. We found that over-expression of p38Kb leads to
93 increased lifespan while loss of p38Kb results in a short lifespan and age-dependent
94 locomotor behavior defects [16]. In addition, oxidatively damaged proteins accumulate in
95 the muscle of p38Kb mutants with age [16], and loss of p38Kb leads to increased
96 polyubiquitination of insoluble proteins and alterations in oxidative stress dependent
97 translation [17], suggesting that these oxidatively damaged proteins may be aggregating in
98 p38Kb mutants. Furthermore, p38Kb has been shown in a *Drosophila* cell culture system
99 to pull down with the HspB8 homologue CG14207 [18], which plays a role in the muscle by
100 regulating protein homeostasis as a part of a protein quality control mechanism called
101 BAG-3 Mediated Selective Autophagy pathway or the Chaperone-Assisted Selective
102 Autophagy (CASA) complex in flies [19,20]. The CASA complex also includes the
103 chaperone Hsc70 and the co-chaperone BAG-3 (starvin in flies). BAG-3/starvin binds to
104 specific damaged or misfolded protein substrates and brings them to the CASA complex

where it binds to Hsc70 and HspB8. Those substrates that cannot be refolded by the complex are polyubiquitinated and targeted to the autophagosome through a handover between BAG-3/stv and the autophagy adaptor protein p62 (ref(2)p in flies), and subsequently degraded through the autophagosome-lysosome system [21–25].

Here, we report that p38Kb regulates age-dependent muscle protein homeostasis through an interaction with the CASA complex. We find that p38Kb acts as an intermediary between BAG-3/starvin and p62/ref(2)p in targeting damaged or misfolded proteins for degradation. This interaction is not only important for maintaining protein homeostasis but also for lifespan extension. In addition, we find that the *Drosophila* homologue of the Hutchinson-Gilford progeria protein, Lamin A/C, is a target for p38Kb and CASA complex mediated protein turnover, suggesting that the p38Kb aging phenotypes may be a result of impaired Lamin degradation.

Materials and Methods

Genotypes

UAS-p38Kb wt, UAS-p38Kb Kinase Dead, p38Kb$^{\Delta 45}$, p38Kb^{Ex41}, w^{1118}, Mef2-GAL4 and MHC-GAL4 were as described in [16]. The p38Kb^{Ex41} is a precise excision allele and serves as a genetic background control for p38Kb$^{\Delta 45}$ deletion mutation.

UAS-stv RNAi 34408 (w^{1118}; P{GD10796}v34408) and UAS-stv RNAi 34409 (w^{1118}; P{GD10796}v34409/TM3) are described in [26] and are from the Vienna Drosophila Resource Center.

131 stv-GFP trap (w^{11118};; Pbac{754.P.F3v30} $stv^{+CPTI\ 002824}$), HspB8-GFP trap (w^{1118}

132 PBac{810.P.FSVS-2}$CG14207^{CPTI004445}$), Hsc70-4 GFP trap (*w^{1118} PBac{544.SVS-*

133 *1}$N^{CPTI002347}$*) are from the Kyoto Stock Center.

134

135 w^{1118}; P{y[+mDint2] w[BR.E.BR]=SUPor-P}ref(2)$P^{KG00926}$, w^{1118};;+mDint2 EY4969 stvEP,

136 Lam^{A25} pr^{1}, and w^{1118}; P{w[+mC]=UAS-Lam.GFP}3-3 were obtained from the

137 Bloomington Drosophila Stock Center.

138

139 All fly stocks were backcrossed into the w^{1118} background and isogenized for 10

140 generations. All stocks were reared at 25ºC in a 12hr:12hr light:dark cycle on standard

141 fly food media.

142

143 **Immunofluorescence**

144 Adult flies were fixed in 4% paraformaldehyde for 48hrs at 4°C. Indirect flight muscles

145 were dissected in 1X PBS, permeabilized in 1X PBS 0.15% Triton-X 100, and blocked in

146 NGS + 0.15% Triton-X 100. Samples were incubated in primary antibody at 4°C

147 overnight, washed in 1X PBS 0.15% Triton-X 100, and incubated in secondary antibody

148 at room temperature for 2hrs. Samples were mounted in Vectashield mounting medium

149 (Vectorlabs) and visualized using a laser scanning confocal microscope. Antibodies:

150 rabbit anti-GFP 1:400 (Invitrogen), mouse anti-FLAG M2 1:1000 (Sigma), rabbit anti-stv

151 1:1000 (gift of Jrög Höhfeld), rat anti-α actinin 1:100 (Abcam), rabbit anti-ubiquitin

152 linkage-specific K63 anti-mouse 1:200 (Abcam), IgG- Alexa Fluor 488 1:200 (Life

153 Technologies), anti-mouse IgG- Alexa Fluor 568 1:500 (Life Technologies), anti-rabbit

154 IgG- Alexa Fluor 488 1:500 (Life Technologies) and Rhodamine Phalloidin 1:2000.

155

156 **Protein aggregate analysis**

157 Indirect flight muscles were prepared as described above from 9 individual flies per
158 genotype. Protein aggregates were identified using mouse anti-polyubiquitin 1:1000
159 (Enzo Life Sciences). Three muscles from each individual fly were imaged as z-series
160 and flattened into a single image as a max projection using confocal microscopy for a
161 total of 27 muscles per genotype. Images were analyzed using Image J "Analyze
162 Particles" function with a diameter of 100 pixels set for the minimum aggregate size.
163 Aggregate number and size were analyzed using ANOVA followed by Tukey's HSD
164 using the R package "multcomp" to generate significance groups with each letter group
165 being significantly different with a p value of ≤ 0.05. Within genotype/across time point
166 analyses were performed using the Welch two sample t-test in R.
167
168 **Lifespan**
169 For lifespan experiments using the UAS-p38Kb^{wt}, ref(2)p -/+, p38Kb$^{\Delta 45/\Delta 45}$, the stv EP
170 (stv^{wt}) lines, and their respective controls, virgin females were kept on standard
171 molasses *Drosophila* media. Due to a change in lab food, the stv RNAi 34408 and stv
172 RNAi 34409 lifespan experiments (with their respective controls) were performed on the
173 standard Bloomington *Drosophila* media. Virgin flies were collected and reared at 25°C
174 in a 12hour:12hour light:dark cycle. Flies were put on new food twice a week. The
175 number of dead animals was scored daily. Lifespan was analyzed using a log rank test
176 to compare genotypes with censored data on all genotypes and then on all pairwise
177 comparisons using the R package "survival" with Benjamini and Hochberg correction
178 (false discovery rate < 0.05).
179
180 **Co-immunoprecipitation**
181 Flies were aged 1 week or 5 weeks. Forty thoraxes per genotype per condition were
182 homogenized in high salt buffer (0.5 M KCl, 35% glycerol,10 mM HEPES pH 7.0, 5 mM

183 $MgCl_2$, 0.5 mM EDTA pH 8.0, 0.1% NP40 25 mM NaF, 1 mM Na_2VO_4, 1 mM DTT,
184 Complete protease inhibitor). The lysate was flash frozen in liquid nitrogen and quickly
185 thawed at 37°C. Then lysates were rocked at 4°C for 30 minutes and centrifuged at
186 14,200 x g for 30 minutes at 4°C. The supernatant was transferred to equilibrated beads
187 anti-Flag (M2) agarose (Sigma) or anti-GFP agarose (Chromotek) and rocked for 2
188 hours at 4°C. Beads were collected using a magnetic bar and washed four times with IP
189 buffer (50 mM HEPES pH 7.0, 100 mM KCl, 0.4% NP40 1.5 mM $MgCl_2$, 5% glycerol, 25
190 mM Na, 1 mM Na_2VO_4, 1 mM EDTA, 1 mM DTT, Complete protease inhibitor). Lysates
191 were then analyzed by immunoblotting using rabbit anti- GFP 1:1000 (Invitrogen),
192 mouse anti-FLAG M2 1:1000 (Sigma), rabbit anti-phospho-p38 1:1000 (Cell Signaling
193 Technologies), goat anti total p38 1:1000 (Santa Cruz Biotechnology), rabbit anti-stv
194 1:10,000 (gift of Jrög Höhfeld) or mouse anti-Lamin 1:1000 (DHSB).
195
196 **Immunoblotting**
197 Wild type flies (w^{1118}) were aged either for 3, 15, 30, and 45 days or for 1-5 weeks. Three
198 thoraxes were dissected and homogenized in 1x Laemmli buffer. Immunoblots were
199 performed as described in [16]. Membranes were developed using SuperSignal West
200 Femto kit (ThermoFisher) or Pierce ECL (ThermoFisher) and exposed on
201 autoradiography film. Antibodies used were: rabbit anti-GFP 1:1000 (Invitrogen), rabbit
202 anti-starvin 1:10,000 (gift of Jrög Höhfeld), mouse anti-actin 1:5,000,000 (Sigma), mouse
203 anti-FLAG M2 (Sigma), rabbit anti-alpha tubulin (Cell Signaling Technologies), mouse
204 anti-Lamin 1:100 (DHSB), rabbit anti-phospho Lamin A Ser22 1:1000 (Thermofisher),
205 mouse anti-beta tubulin (E-10) 1:5000 (Santa Cruz Biotechnology), mouse anti- HRP
206 1:20,000 (Jackson Labs), rabbit anti-HRP 1:40,000 (Jackson Labs). Densitometry was
207 performed using a minimum of three independent blots. For statistical analysis of protein

208 expression level, pixel density of the tested protein was normalized within sample to the
209 loading control. These values were then normalized to control to calculate fold change.
210 The fold change values were analyzed by Student's t-test or ANOVA [27] as appropriate.
211
212 **Sucrose Gradient Fractionation**
213 p38Kb$^{Ex41/Ex41}$ and p38Kb$^{\Delta45/\Delta45}$ flies were aged three weeks. 30 thoraxes per genotype
214 were dissected and homogenized in NP40 lysis buffer. Samples were centrifuged at
215 800xg for 10 minutes at 4°C. The supernatant was then transferred to a 15-50% sucrose
216 discontinuous gradient. Samples were then ultracentrifuged at 55,000 rpm (201,000xg at
217 r_{av}) for 20 hours at 4°C in a TLS-55 in a Beckman Coulter Optima TLX Ultracentrifuge.
218 200μl fractions were collected and the pellet was resuspended in an equal volume of
219 NP40 Lysis Buffer.
220
221 **Stv localization**
222 Immunohistochemistry on p38Kb$^{Ex41/ Ex41}$ and p38Kb$^{\Delta45/\Delta45}$ Indirect flight muscles was
223 performed as described above. Confocal images from five individual flies per genoytpe
224 were analyzed for average pixel density using ImageJ in three different non-overlapping
225 locations on each muscle for a total of 15 measurements per genotype. Average pixel
226 density was analyzed by Student's t-test using R.
227
228 **Results**
229
230 **p38Kb regulates age-dependent protein homeostasis.**
231 p38Kb null mutant animals (p38Kb$^{\Delta45/\Delta45}$, a deletion of the p38Kb gene) exhibit age-
232 dependent locomotor behavior defects and have a 48% lifespan reduction. In addition,

233 biochemical analysis suggests that p38Kb null mutants have increased levels of
234 insoluble polyubiquitinated proteins in the thoracic musculature of aged animals as
235 observed by immunoblot analysis [17]. However, protein aggregate size and distribution
236 have not been visualized in the p38Kb mutants, nor is it known whether augmenting
237 p38Kb activity in muscles leads to a change in protein homeostasis. Therefore, we
238 analyzed how p38Kb expression influences protein aggregation. We find that p38Kb null
239 mutants have an increased number of protein aggregates in the adult indirect flight
240 muscle at 1 week and 3 weeks of age (Figure 1A-B and E-F, Table S1) and increased
241 aggregate size with age (Figure 1G-H, Table S1) as compared to a genetic background
242 control ($p38Kb^{Ex41/Ex41}$, a precise excision allele). Furthermore, transgenic inhibition of
243 p38Kb in the muscle using a dominant negative kinase dead construct ($p38Kb^{KD}$, [16]) also
244 results in a significant increase in aggregate number, however aggregate size was not
245 affected (Figure 1I-L and Table S2). Conversely, as both strong and moderate levels of
246 p38Kb over-expression lead to an increased lifespan (37% and 14% extension,
247 respectively) [16], we tested if p38Kb over-expression also affects protein aggregation. We
248 find that both strong over-expression of p38Kb in the adult muscle using the Mef2-GAL4
249 driver (Figure 1C-D and M-P, Table S3) and moderate over-expression of p38Kb using
250 the MHC-GAL4 driver (Figure 1Q-T and Table S4) leads to decreased protein aggregate
251 number and size throughout the lifespan. It has been hypothesized that protein
252 aggregate accumulation and increased size may be toxic, potentially explaining the
253 decreased lifespan and age-dependent locomotor abnormalities in $p38Kb^{\Delta 45}$ null mutants
254 and the increased longevity in the p38Kb over-expression animals.
255
256 **p38Kb mediates age-dependent phenotypes through autophagy**
257 In order to determine what mechanism plays a role in the clearance of polyubiquitinated
258 protein aggregates, we first tested what type of ubiquitin linkage is present in the

259 aggregates in wild type flies. In particular, K63-linked ubiquitination has been shown to
260 facilitate the formation of aggregates [28–30] that are cleared through autophagy [30–32]. We
261 find that a subset of aggregates from aging flies contain K63-linked ubiquitinated
262 proteins (Figure 2A-C), suggesting that these muscle protein aggregates are degraded
263 through autophagy. Polyubiquitinated protein aggregates can be degraded through
264 selective autophagy in which the adaptor protein p62 (ref(2)p in flies) promotes the
265 packaging and delivery of polyubiquitinated proteins to the autophagosome [33]. If p38Kb
266 requires selective autophagy to mediate protein homeostasis, then loss of ref(2)p will
267 block the p38Kb mediated decreased aggregation phenotype. We find that loss of a
268 single copy of *ref(2)p* results in fewer aggregates (Figure 2D-E and Table S5), which
269 may reflect compensation by other protein clearance mechanisms with aging, especially
270 as homozygous *ref(2)p* mutants are viable. When a single copy of *ref(2)p* is removed in
271 the p38Kb over-expression background, this prevents the reduced protein aggregation
272 observed in the p38Kb over-expression animals at both young and old ages (Figure 2D-
273 E and Table S5). This dominant interaction suggests that *ref(2)p* acts downstream of
274 p38Kb to promote the degradation of protein aggregates.
275
276 **p38Kb colocalizes with the CASA complex in the adult flight muscle.**
277 In order to better understand the role of p38Kb in protein homeostasis, we first
278 determined where in the muscle p38Kb localizes and find that a FLAG-tagged p38Kb
279 (green) colocalizes with the Z-disc marker alpha-actinin and is also present at the M-line
280 (Figure 2F). The muscle Z-disc is an area of high protein turnover, and one protein
281 quality control mechanism that localizes to the Z-disc in mice and adult flies is the
282 Chaperone-Assisted Selective Autophagy (CASA) complex [19,34]. In adult *Drosophila*
283 muscle, the CASA complex has been reported to consist of the Hsc70 homologue,
284 Hsc70-4, the HspB8 homologue CG14207 and the BAG-3 homologue starvin (stv) [19].

285 We find that p38Kb colocalizes with all the CASA complex members at the Z-disc and
286 M-line (Figure 2G-I).
287
288 **p38Kb physically interacts with the CASA complex in the adult flight muscle.**
289 In order to further determine if p38Kb physically interacts with the CASA complex in the
290 adult muscle, we performed co-immunoprecipitation experiments. In *Drosophila* cell
291 culture p38Kb^{wt} was shown to co-immunoprecipitate with the HspB8 homologue
292 CG14207[18], therefore, we tested if this interaction also occurs in adult indirect flight
293 muscle. As the interaction between p38Kb and its targets may be transient, we utilized a
294 FLAG-tagged p38Kb kinase dead construct (UAS-p38Kb^{KD} Mef2-GAL4) that is able to
295 be activated and bind to a target but cannot phosphorylate it, leading to a delayed
296 release of the target[35]. We expressed p38Kb^{KD} in the adult flight muscle of a fly that also
297 endogenously expressed GFP tagged HspB8, in which GFP is spliced in as a new exon
298 of the endogenous gene. This results in a GFP fusion protein that is expressed in the
299 same pattern as endogenous HspB8 ([19] and Figure 2H'). We find that p38Kb^{KD} was able
300 to pull down HspB8 (Figure 2J) as compared to the HspB8-GFP control background. In
301 addition, expression of p38Kb^{KD} in a wildtype background was able to pull down un-
302 tagged endogenous stv (Figure 2K). We then performed reverse IPs in which we
303 immunoprecipitated each endogenously GFP tagged CASA complex protein (Hsc70-4,
304 HspB8, or stv) and probed for FLAG tagged p38Kb^{KD} and found that p38Kb co-
305 immunoprecipitates with the CASA complex (Figure 2L-N) with stronger binding at
306 younger ages than older ages. Interestingly, we found no significant difference in the
307 expression levels of Hsc70-GFP, stv-GFP, and over-expression of p38Kb^{KD} with age
308 (Figure S1A-B, D) while levels of HspB8-GFP increased with age (Figure S1C). These
309 data suggest that the age-dependent interaction between p38Kb and the CASA complex

310 may be due to changes in the physical interactions between these proteins rather than a
311 reduction in protein levels.
312 To verify that endogenous p38Kb can interact with the CASA complex, we
313 performed co-immunoprecipitations with muscle lysates from flies expressing either
314 endogenously GFP tagged Hsc70-4, HspB8 or stv in a wild type background and probed
315 for endogenous activated p38K that is dual phosphorylated on the TGY motif. We find
316 that all three members of the CASA can co-immunoprecipitate with endogenous
317 phosphorylated p38K in the muscle (Figure 2O). These results suggest that p38Kb is
318 able to physically interact with the CASA complex.
319
320 **p38Kb acts downstream of the CASA complex.**
321 As p38Kb physically interacts with the CASA complex, we next tested if p38Kb is
322 acting upstream activity of the complex to promote the initial recognition of misfolded
323 proteins or the downstream activity of the complex to direct un-foldable proteins to the
324 autophagosome. As BAG-3/stv provides both the specificity to the CASA complex and is
325 involved in the handoff of damaged proteins to p62/ref(2)p for autosomal degradation [21–
326 25], we tested for genetic interactions between p38Kb and *stv*. *stv* null mutants have
327 impaired locomotor functions, muscle degeneration and early lethality [19,36]. Due to the
328 severity of these null phenotypes, we utilized *stv* RNAi lines to generate an allelic series
329 of *stv* loss of function in the muscle. We find that weak inhibition of stv (UAS-stv
330 RNAi^{34408} MHC-GAL4) had no effect on protein aggregation (Table S6). However,
331 moderate inhibition of stv (UAS-stv RNAi^{34409} MHC-GAL4) results in increased protein
332 aggregate number and size (Figure 3A-B and Table S7) and results in a decrease in
333 lifespan particularly in the first half of life as compared to outcrossed controls (Figure 3C
334 and Table S8). Strong inhibition of *stv* (UAS-stv RNAi^{34408} Mef2-GAL4) leads to a
335 severely reduced lifespan of ~4 days on average (Figure 3D and Table S9).

336 If p38Kb acts to regulate the downstream activity of the CASA complex, then over-
337 expression of p38Kb should rescue these *stv* RNAi phenotypes. We find that over-
338 expression of p38Kb rescues both protein aggregate number and size in the *stv*
339 moderate inhibition background (Figure 3A-B and Table S7) and also rescues the
340 lifespan defect (Figure 3C and Table S9). Furthermore, p38Kb over-expression is able to
341 partially rescue the decreased lifespan exhibited by strong *stv* inhibition increasing
342 average lifespan from 4 days to 13 days (Figure 3D and Table S10). To further test if
343 p38Kb acts downstream of the CASA complex, we combined loss of p38Kb with CASA
344 complex over-expression. If p38Kb acts downstream of the CASA complex, then over-
345 expression of the CASA complex members in the p38Kb mutant background will not be
346 able to rescue the p38Kb mutant phenotypes. We find that over-expression of stv in the
347 p38Kb mutants not only fails to rescue the p38Kb mediated short lifespan defect but
348 reduces the lifespan further (Figure 3E and Table S11). This is particularly striking as
349 over-expression of stv in a wild type background does not significantly affect lifespan
350 (Figure 4H and Table S12) as compared to the outcrossed transgene control (p value =
351 0.195). This suggests that p38Kb may be a limiting factor in regulating the downstream
352 activity of the CASA complex in which it hands the poly-ubiquitinated misfolded proteins
353 to ref(2)p for degradation through the autophagosome.
354
355 **p38Kb regulates the activity of the CASA complex in protein homeostasis.**
356 If p38Kb is a limiting factor for stv function, then the combined over-expression of
357 p38Kb and stv may result in a further beneficial effect. We find that over-expression of
358 stv alone results in fewer aggregates at young and old ages (Figure 4A-B and Table
359 S13) and smaller aggregates with age (Figure 4D and Table S13) as compared to
360 outcrossed controls. However, co-over-expression of p38Kb and stv does not result in a
361 further reduction in aggregate number as compared to over-expression of p38Kb or stv

362 alone (Figure 4A and Table S13). By 5 weeks of age, co-over-expression of p38Kb and
363 stv flies have comparable aggregate number to controls (Figure 4B and Table S13).
364 Conversely, p38Kb and stv co-over-expression results in a reduction in aggregate size at
365 a young age compared to over-expression of stv alone (Figure 4C and Table S13, p
366 value < 0.001), suggesting that p38Kb is a limiting factor for stv function in regulating
367 aggregate size. Unlike with aggregate number, the aggregates remain significantly
368 smaller in size as the flies age in the combined over-expression background (Figure 4D
369 and Table S13). We also find that co-over-expression of p38Kb and stv leads to an
370 additional 5% increase in lifespan relative to p38Kb over-expression alone (Figure 4H
371 and Table S12). Interestingly, the co-over-expression animals show a very similar
372 lifespan to the p38Kb over-expression alone animals until ~day 50, when the p38Kb
373 alone animals begin to die at a faster rate (Figure 4H). One explanation is that co-over-
374 expression of p38Kb and stv provides beneficial effects in early adulthood that continue
375 throughout adulthood leading to increased lifespan despite the presence of protein
376 aggregates. Another possibility is that aggregate size is a reflection of aggregate
377 content. If the CASA complex can only target a subset of proteins for refolding or
378 degradation, then increasing CASA complex activity could lead to smaller aggregates as
379 the CASA targets are effectively degraded through an interaction with p38Kb and ref(2)p
380 rather than aggregating. Therefore, size and/or content may play a more important role
381 in determining lifespan as compared to overall aggregate number.
382
383 **p38Kb is required for proper localization of stv in the muscle.**
384 Since we find that p38Kb acts between stv and ref(2)p in regulating protein
385 aggregation, we hypothesize that p38Kb plays a role in stabilizing the transfer of
386 misfolded proteins primed for degradation from the CASA complex to ref(2)p. If so, then
387 over-expression of p38Kb would lead to increased efficiency in targeting misfolded

388 proteins to the autophagosome (Figure 1M-T), and inhibition of p38Kb would lead to an
389 increase in protein aggregation (Figure 1E-L). In addition, loss of p38Kb may lead to a
390 failure of stv to maintain its interaction with the CASA complex or to interact with ref(2)p.
391 Therefore, we tested if stv is still able to localize to the Z-disc in the absence of p38Kb.
392 We find that in p38Kb null mutants, stv is more diffuse throughout the muscle but is still
393 able to localize to the Z-disc and M-line in (Figure 4E-G), suggesting that its localization
394 is partially impaired in the absence of p38Kb. Furthermore, we find that the localization
395 of the CASA complex member HspB8 in the muscle is unaffected by loss of p38Kb
396 (Figure S2). These data indicate that p38Kb may play a role in stabilizing the interaction
397 between the CASA complex and stv that allows stv to direct misfolded proteins to
398 ref(2)p.
399
400 **Lamin protein binds to the CASA complex and accumulates in stv RNAi and**
401 **p38Kb mutants.**
402 In order to determine if p38Kb might be playing a role in the targeting of
403 misfolded proteins from stv to ref(2)p, we first needed to identify a protein target of both
404 stv and p38Kb. Therefore, we focused on proteins associated with Limb-Griddle
405 Muscular Dystrophy (LGMD), which is caused by mutations in either BAG-3 (stv) or
406 HspB8 [37–39]. In addition, p38K signaling has been implicated in LGMD [40–42]. *Drosophila*
407 have 19 orthologues of LGMD proteins, one of which is Lamin A/C (Lamin or Lamin Dm0
408 in flies). Lamin is of particular interest since mutations in Lamin A/C also result in the
409 accelerated aging disorder Hutchinson-Gilford progeria [43–45], and Lamin has been shown
410 to aggregate under oxidative stress conditions [46]. Mutations in Lamin A/C are also
411 sufficient to induce Lamin aggregation and abnormal nuclear morphology in human cell
412 culture, *C. elegans*, and *Drosophila* systems [44,47–54]. Furthermore in *Drosophila*, Lamin

413 knockouts have similar phenotypes to p38Kb and/or stv mutants, such as reduced
414 locomotor function and increased activity of the Nrf-2/Keap-1 pathway [49,55,56].
415 If Lamin is a target of the CASA complex, then decreased activity of the CASA
416 complex should result in an accumulation of Lamin protein. We find that Lamin levels do
417 not change with age (Figure 5A), however, inhibition of stv results in a significant
418 increase in the total amount of Lamin protein regardless of age (Figure 5A-B, p value
419 0.028). Interestingly, loss of p38Kb leads to an age-dependent increase in Lamin protein
420 as compared to age matched controls (Figure 5C-D, p value = 0.006643). As the
421 association between p38Kb and the CASA seems to decline with age (Figure 2L-N),
422 these data suggest that p38Kb activity later in life is important for maintaining protein
423 homeostasis and lifespan.
424 To investigate if Lamin is accumulating in the protein aggregates, we performed
425 fractionation experiments in which we find that Lamin is predominantly found in fractions
426 5-7 in controls with the majority concentrated in faction 6 (Figure 5E). Interestingly, we
427 also find a high molecular weight from of Lamin mainly restricted to fraction 5 (Figure
428 5E). In addition, we also observe that both the main and high molecular weight Lamin
429 species are in the aggregate containing pellet (Figure 5E). We next tested how loss of
430 p38Kb affects the aggregation of Lamin and find that p38Kb mutants have decreased
431 Lamin in fractions 5-7 with a concurrent increase of both the main and high molecular
432 weight species of Lamin in the pellet (Figure 5E). This suggests that Lamin is a target of
433 p38Kb and that loss of p38Kb results in increased aggregation of Lamin.
434
435 Of interest is this high molecular weight form of Lamin, which is present in
436 fraction 5 and the aggregates (Figure 5E). One important protein domain in Lamin is the
437 CaaX box, which is farnesylated and required for Lamin localization to the inner nuclear
438 membrane[57–60]. To test if this might be a farnesylated form of Lamin, we utilized the

439 Lam^{A25} mutant which has a frameshift that results in the loss of the C-terminal CaaX
440 box[61]. We find that the high molecular weight form of Lamin is lost in the Lam^{A25} mutant
441 whereas the predominant 75kDa band of Lamin is still present (Figure 5F). These data
442 suggest that the high molecular weight Lamin we observe is the farnesylated form.
443
444 In addition to farnesylation, Lamin can also be phosphorylated by a variety of
445 kinases that can change the solubility of Lamin [54,62]. For example, in a *Drosophila* cell
446 culture system, a phospho-mimic mutation at Ser45 (the equivalent of Ser22 in humans)
447 results in Lamin aggregation in both the nucleus and cytoplasm [54]. This serine residue is
448 phosphorylated by the cd2 kinase [63], but also happens to be a potential p38K
449 phosphorylation site. Therefore, we tested if the levels of phospho- Ser45 Lamin are
450 altered in p38Kb mutants. We find that phospho-Lamin levels are not significantly altered
451 in the p38Kb mutants (Figure 5G-H p=0.09), suggesting that p38Kb is not required for
452 Ser45 phosphorylation. We next examined if phosphorylated Lamin is also present in the
453 aggregates. We find that in controls, phosphorylated Lamin is present in factions 5-7
454 with low amounts in the pellet (Figure 5I). We also observe a low molecular weight
455 phospho-Lamin form that appears in the pellet (Figure 5I). In the p38Kb mutants,
456 phospho-Lamin expression is reduced in fractions 6 and 7 and accumulates in the pellet
457 (Figure 5I). Furthermore, increasingly smaller low molecular weight species of phospho-
458 Lamin are present in the $p38Kb^{\Delta 45}$ mutants including the pellet (Figure 5I), suggesting
459 that loss of p38Kb prevents the effective clearance of these Lamin cleavage forms.
460 Interestingly, loss of the Lamin CaaX box does not affect these lower molecular weight
461 forms, however, it does result in an increase in the phosphorylation of full-length Lamin
462 (Figure 5F). Additionally, we do not detect phosphorylation positive high molecular
463 weight forms of Lamin (Figure 5F), suggesting that farnesylated lamin is not
464 phosphorylated at Ser45. These data combined with our finding that full length Lamin is

465 phosphorylated, suggest that when Lamin is unphosphorylated it is prone to
466 farnesylation that may lead to aggregation.
467
468 To determine if Lamin is a direct target of p38Kb and the CASA complex, we
469 tested if Lamin can bind to the CASA complex. We immunoprecipitated endogenously
470 GFP tagged HspB8, Hsc70-4 and stv from adult *Drosophila* muscle and probed for
471 endogenous Lamin. We find that full-length Lamin co-immunoprecipitates with all three
472 members of the CASA complex (Figure 6A), but do not detect binding with either the
473 higher or lower molecular weight forms of Lamin found in the fractions (Figure 5E and I).
474 Furthermore, we expressed either a nuclear localization signal tagged GFP or Lamin
475 tagged with GFP in the muscle and found that endogenous stv co-immunoprecipitates
476 with Lamin (Figure 6B). These data suggest that the CASA complex is able to bind to
477 misfolded forms of full-length Lamin for targeting to the autophagosome.
478
479 As we hypothesize that p38Kb is interacting with the CASA complex at the point
480 in which the misfolded targets are handed over to ref(2)p for degradation, we tested if
481 p38Kb also binds to Lamin. We find that p38Kb^{KD} expressed in the muscle co-
482 immunoprecipitates with both high and low molecular weight forms of Lamin (Figure 6C).
483 Interestingly, p38Kb physically interacts with the aggregate prone low molecular weight
484 species of Lamin as opposed to the predominant full-length form of Lamin (Figure 6C).
485 More striking is that p38Kb^{KD} physically interacts with increasingly larger forms of Lamin
486 (Figure 6C), suggesting that p38Kb is interacting with the poly-ubiquitinated forms of
487 Lamin.
488
489 We have developed a model in which misfolded proteins are targeted by stv to
490 the CASA complex. Those proteins that cannot be refolded are then tagged with poly-

491 ubiquitin. These poly-ubiquitinated proteins are handed off to ref(2)p in a process
492 mediated by p38Kb. This model predicts that in p38Kb mutants these poly-ubiquitinated
493 proteins accumulate and then form aggregates. It additionally predicts that over-
494 expression of p38Kb would lead to increased efficiency of the poly-ubiquitinated proteins
495 being targeted to the autophagosome. This model would also predict that misfolded full-
496 length Lamin would bind to the CASA complex for refolding. If Lamin cannot be refolded
497 it is then poly-ubiquitinated and transferred to ref(2)p through an interaction with p38Kb.
498

499 **Discussion**

500 We find that the aging gene p38Kb regulates age-dependent protein homeostasis
501 through an interaction with the CASA complex and is acting at a step between the poly-
502 ubiquitination of a un-foldable target and its transfer to ref(2)p for autolysosomal
503 mediated degradation. Interestingly, we find that p38Kb is important for the proper
504 localization of stv to the Z-disc but does not affect the localization of other complex
505 members. This suggests that p38Kb may play a role in maintaining the interaction
506 between stv and the CASA complex which may be necessary for target transfer to
507 ref(2)p. stv has a conserved MAPK docking site as well several potential conserved
508 p38K phosphorylation sites. Furthermore, mammalian p62 has been shown to bind to
509 p38Kb in vitro through two domains [64], which are partially conserved in flies. Therefore,
510 one possibility is that p38Kb mediated phosphorylation of stv facilitates the localization of
511 a functional CASA complex to the Z-disc, where damaged proteins are rapidly turned
512 over. Another possibility is that p38Kb binds to stv and ref(2)p and that the
513 phosphorylation of stv is required for target hand-over to ref(2)p so that in the absence of
514 p38Kb, stv cannot transfer targets to ref(2)p. A consequence of this may be that stv and
515 the protein target together are released from the CASA complex, leading to
516 mislocalization of stv. As we don't detect a decrease in phospho-Lamin in the p38Kb

517 mutants or find that the p38Kb can pull-down phospho-Lamin, it is unlikely that p38Kb is
518 directly phosphorylating the target proteins as a part of the stv-ref(2)p hand-over
519 process.
520
521 How protein aggregation contributes to aging and disease has been an area of
522 great interest. One outstanding question is if protein aggregation is a consequence or
523 cause of aging. It has been hypothesized that protein aggregates accumulate with age
524 as the amount of damaged or misfolded proteins increase. However, it is not clear
525 whether or not these aggregating proteins are toxic leading to tissue dysfunction and a
526 disease state. Previous studies have found that long-lived fly strains such as over-
527 expression of Foxo or parkin result in reduced protein aggregate formation [4,65].
528 Therefore, we hypothesized that decreased protein aggregation would lead to improved
529 measures of healthspan, while increased protein aggregation would lead to reduced
530 measures of healthspan. As expected, we find that the short-lived p38Kb mutants, which
531 exhibit premature locomotor behavior defects [16], have large and numerous protein
532 aggregates. Similarly, inhibition of stv results in increased aggregation and decreased
533 lifespan. We also find that over-expression of p38Kb leads to decreased protein
534 aggregation and increased lifespan. However, over-expression of stv leads to decreased
535 aggregate number but does not extend lifespan. One possibility is that decreasing
536 aggregation alone is not sufficient to promote lifespan extension. Another possibility is
537 that aggregate number is not as critical as aggregate size and/or content, particularly
538 early in life, for lifespan extension. We find that stv over-expression only results in
539 decreased aggregate size in older animals, however, co-over-expression of p38Kb and
540 stv leads to reduced aggregate size at a young and old ages and leads to a further
541 increase in lifespan. Thus, the turnover of specific toxic protein or subset of proteins
542 early in life may lead to a reduction in the exposure to these toxic species and a lifespan

543 extension. We find that Lamin, which is mutated to an aggregation prone protein form in
544 Hutchinson-Gilford progeria [44,53,62,66], is a target of p38Kb and the CASA complex.
545 Interestingly, p38Kb and Lamin mutants share similar phenotypes such as age-
546 dependent locomotor impairments [16,55,56] and upregulation of the Nrf-2/Keap-1 pathway
547 [16,49]. As loss of p38Kb leads to an accumulation of Lamin in the aggregates, this may be
548 toxic to the cell, leading to impaired locomotor function, increased stress and decreased
549 lifespan. Thus, we have found that one aging gene (p38Kb) regulates a second,
550 unrelated aging gene (Lamin) via the CASA complex. These data suggest a new link
551 between aging pathways and how they may converge through the regulation of protein
552 homeostasis.
553

554 **Acknowledgements**

555 We would also like to acknowledge the Bloomington Drosophila Stock Center (NIH
556 P40OD018537), the Vienna Drosophila Resource Center, and Kyoto Stock Center for
557 providing fly stocks used in this study. A. Vrailas-Mortimer was funded by start-up funds
558 from the University of Denver, a Knoebel Center for the Study of Aging pilot grant, start-
559 up funds from Illinois State University and was supported by the National Institute of
560 Arthritis and Musculoskeletal and Skin Diseases of the National Institutes of Health
561 under Award Number R15AR070505. The content is solely the responsibility of the
562 authors and does not necessarily represent the official views of the National Institutes of
563 Health. S. Sanyal was funded by startup funds from Emory University. S. Ryan was
564 supported by a Knoebel Center for the Study of Aging pilot grant to A. Vrailas-Mortimer
565 and S. Barbee, N. Mortimer was funded by start-up funds from Illinois State University.
566 The funders had no role in study design, data collection and analysis, decision to
567 publish, or preparation of the manuscript.
568

569

570 **Figure Legends**

571

572 **Fig 1. p38Kb regulates age-dependent protein homeostasis.**

573 Confocal micrographs of polyubiquitin positive protein aggregates in the adult indirect

574 flight muscle in **A)** a precise excision genetic background control p38Kb$^{Ex41/\ Ex41}$ and **B)**

575 p38Kb $^{\Delta45/\Delta45}$ null mutants at three weeks of age and in **C)** outcrossed Mef2-GAL4

576 controls (Mef2>w^{11118}) and **D)** UAS-p38Kb^{wt} Mef2-GAL4 (Mef2>p38Kb^{wt}) over-expression

577 animals at 5 weeks of age. Scale bar equals 6.2 μm. Box-Whisker plots of aggregate

578 number in p38Kb $^{\Delta45/\Delta45}$ mutants as compared to p38Kb$^{Ex41/Ex41}$ controls at **E)** 1 week and

579 **F)** 3 weeks of age and aggregate size at **G)** 1 week and **H)** 3 weeks of age. Aggregate

580 number in p38Kb^{KD} Mef2-GAL4 (Mef2>p38Kb^{KD}) and outcrossed Mef2-GAL4 controls at

581 **I)** 1 week and **J)** 5 weeks of age and aggregate size at **K)** 1 week and **L)** 5 weeks of

582 age. Aggregate number in strong p38Kb over-expression animals and outcrossed Mef2-

583 GAL4 controls at **M)** 1 week and **N)** 5 weeks of age and aggregate size at **O)** 1 week

584 and **P)** 5 weeks of age. Aggregate number in moderate p38Kb over-expression

585 (MHC>p38Kb^{wt}) animals and outcrossed MHC-GAL4 controls (MHC>w^{1118}) at **Q)** 1 week

586 and **R)** 5 weeks of age and aggregate size at **S)** 1 week and **T)** 5 weeks of age.

587

588 **Fig 2. p38Kb regulates aging phenotypes through ref(2)p.**

589 **A-C)** A subset of polyubiquitinated protein aggregates (green) in 3 week old

590 p38Kb^{Ex4}/^{Ex41} control muscle contain K63 ubiquitinated (magenta) proteins (white

591 arrows). **D-E)** Protein aggregate number in ref(2)p heterozygous mutant backgrounds at

592 **D)** 1 week and **E)** 5 weeks. Loss of a single copy of ref(2)p prevents the p38Kb mediated

593 reduced protein aggregation at 1 week and 5 weeks of age. Asterisks denote a p-value

594 of ≤0.001. **(F-I)** Localization of a FLAG-tagged p38Kb (green in **F-I** and **F''-I''**) in the

595 adult indirect flight muscle. **F)** FLAG-tagged p38Kb localizes to the Z-disc (arrows) as
596 exhibited by colocalization with the Z-disc protein alpha-actinin (magenta, **F'** and **F''**), as
597 well as the M-line (arrowheads). **G-I)** p38Kb colocalizes with each CASA complex
598 member (magenta, **G'-I'**) at the Z-disc. Over-expression of a FLAG tagged p38Kb in the
599 muscle in **G**) an endogenous Hsc70-GFP fusion protein background, **H**) an endogenous
600 HspB8-GFP fusion protein background, and **I)** a wildtype background with endogenous
601 levels of stv. **J-K)** Muscle lysates expressing control and Mef2-GAL4 UAS-p38Kb$^{KD\text{-}FLAG}$
602 in either **J)** an endogenously expressed HspB8-GFP background or **K)** a wildtype
603 background were immunoprecipitated using anti-FLAG coated beads. **J)** Immunoblots
604 were probed with anti-GFP to detect the presence of HspB8 in the IP lysates or with **K)**
605 anti-stv to detect the presence of stv in the IP lysates. **L-N)** Muscle lysates expressing
606 p38Kb $^{KD\text{-}FLAG}$ in an endogenously expressed **L)** Hsc70-GFP, **M)** HspB8-GFP and **N)** stv-
607 GFP background were immunoprecipitated using anti-GFP coated beads. Immunoblots
608 were probed with anti-FLAG to detect the presence of p38Kb in the IP lysates. Note: stv
609 is tagged with both GFP and FLAG. **O)** Endogenous phospho-p38 co-
610 immunoprecipitates with Hsc70-4-GFP, HspB8-GFP, and stv-GFP. Muscle lysates were
611 immunoprecipitated with anti-GFP beads, and immunoblots were probed with anti-
612 phospho-p38K.
613
614 **Fig 3. p38Kb genetically interacts with stv to regulate protein homeostasis and**
615 **lifespan. A)** Protein aggregate number and **B)** size in the moderate stv knockdown
616 background using MHC-GAL4 at 5 weeks. Asterisks denote a p-value of ≤0.001. **C)**
617 Moderate over-expression of p38Kb (red line) results in an increased lifespan as
618 compared to the MHC-GAL4 controls and p38Kb transgene control (black line and gray
619 lines, respectively). Moderate knockdown of stv using the MHC-GAL4 results in a
620 decreased lifespan (pink line compared to yellow and black lines) and is rescued by

621 p38Kb over-expression (compare pink line to blue line). **D)** Strong over-expression of
622 p38Kb (red line) results in an increased lifespan as compared to the Mef2-GAL4 controls
623 and p38Kb transgene control (black line and gray lines, respectively). Strong knockdown
624 of stv using the Mef2-GAL4 results in a decreased lifespan (pink line compared to yellow
625 and black lines) and is partially rescued by p38Kb over-expression (compare pink line to
626 blue line). **E)** Over-expression of stv in the p38Kb mutant background results in a further
627 reduction of lifespan as compared to p38Kb mutant controls (compare blue line to red
628 and grey lines).
629
630 **Fig 4. p38Kb is limiting for stv function and localization.**
631 Protein aggregate number at **A)** 1 week and **B)** 5 weeks and protein aggregate size at
632 **C)** 1 week and **D)** 5 weeks measured in stv over-expression backgrounds. Over-
633 expression of stv leads to reduced aggregate number at 1 and 5 weeks and aggregate
634 size at 5 weeks. Co-over-expression of stv and p38Kb does not result in a further
635 decrease in protein aggregate number but trends towards decreased aggregate size at
636 both 1 and 5 weeks of age. Asterisks denote a p-value of ≤0.001 when compared to the
637 GAL4 control. **E)** stv localizes to the adult muscle Z-disc and M-line (white arrows) in
638 control animals. **F)** stv localization is disrupted in p38Kb mutants. **G)** Quantification of
639 average pixel density. **H)** Over-expression of stv alone has no significant effect on
640 lifespan (pink line as compared to yellow and black lines), however, co-over-expression
641 of stv and p38Kb results in a further increase in lifespan (compare red line to blue line).
642
643
644 **Fig 5. p38Kb and stv regulate Lamin aggregation.**
645 **A)** Immunoblot analysis of stv-RNAi and GAL4 controls flies muscle lysates probed with
646 anti-Lamin and **B)** quantified using densitometry. **C)** Immunoblot analysis of

647 p38Kb$^{Ex41/Ex41}$ control and p38Kb $^{\Delta45/\Delta45}$ mutant muscle lysates probed with anti-Lamin
648 and **D)** quantified using densitometry. **H)** Immunoblots of sucrose gradient fractions
649 from 3 week old p38Kb$^{Ex41/Ex41}$ control and p38Kb $^{\Delta45/\Delta45}$ mutant muscle probed with anti-
650 Lamin. **G)** Immunoblot analysis of p38Kb$^{Ex41/Ex41}$ control and p38Kb $^{\Delta45/\Delta45}$ mutant muscle
651 lysates probed with anti-phospho Lamin and **H)** quantified using densitometry. **I)**
652 Immunoblots of sucrose gradient fractions from 3 week old p38Kb$^{Ex41/Ex41}$ control and
653 p38Kb $^{\Delta45/\Delta45}$ mutant muscle probed with anti-phospho-Lamin.
654
655 **Fig 6. p38Kb and stv physically interact with Lamin.**
656 **A)** Endogenous HspB8-GFP, Hsc70-GFP and stv-GFP-FLAG fusion proteins were
657 immunoprecipitated from adult muscle lysate using anti-GFP coated beads.
658 Immunoblots were probed with anti-Lamin and anti-GFP. **B)** A nls-GFP or Lamin-GFP
659 was expressed in muscles using MHC-GAL4. GFP proteins were immunoprecipitated
660 from adult muscle lysates using anti-GFP coated beads. Immunoblots were probed with
661 anti-stv and anti-GFP. C) p38Kb^{KD} was expressed in muscles using Mef2-GAL4. p38Kb
662 was immunoprecipitated from adult muscle lysates using anti-FLAG coated beads.
663 Immunoblots were probed with anti-lamin and anti-FLAG.
664
665 **Fig S1. CASA complex expression with age.** Immunoblot analysis of **A)** endogenously
666 GFP tagged Hsc70-4, **B)** endogenously GFP tagged HspB8, **C)** stv, and **D)** the FLAG
667 tagged p38Kb kinase dead transgene with age. Asterisks denote a p value of ≤0.05 as
668 compared to the 3 day time point.
669
670 **Fig S2. Localization of HspB8 in p38Kb mutants.** Endogenously GFP-tagged HspB8
671 was analyzed in the muscle of three week old **A)** controls and **B)** p38Kb mutants. HspB8

672 (green) localizes to the Z-disc and M-line of the indirect flight muscle (actin in magenta)
673 in both control and p38Kb mutant animals.
674
675
676 **References**

677 1. Taylor, R. C. & Dillin, A. Aging as an event of proteostasis collapse. *Cold Spring*
678 *Harb. Perspect. Biol.* **3**, (2011).
679 2. Ben-Zvi, A., Miller, E. A. & Morimoto, R. I. Collapse of proteostasis represents an
680 early molecular event in Caenorhabditis elegans aging. *Proc. Natl. Acad. Sci. U. S.*
681 *A.* **106**, 14914–14919 (2009).
682 3. Cohen, E., Bieschke, J., Perciavalle, R. M., Kelly, J. W. & Dillin, A. Opposing
683 activities protect against age-onset proteotoxicity. *Science* **313**, 1604–1610 (2006).
684 4. Demontis, F. & Perrimon, N. FOXO/4E-BP signaling in Drosophila muscles regulates
685 organism-wide proteostasis during aging. *Cell* **143**, 813–825 (2010).
686 5. Morley, J. F., Brignull, H. R., Weyers, J. J. & Morimoto, R. I. The threshold for
687 polyglutamine-expansion protein aggregation and cellular toxicity is dynamic and
688 influenced by aging in Caenorhabditis elegans. *Proc. Natl. Acad. Sci. U. S. A.* **99**,
689 10417–10422 (2002).
690 6. Palazzolo, I. *et al.* Overexpression of IGF-1 in muscle attenuates disease in a mouse
691 model of spinal and bulbar muscular atrophy. *Neuron* **63**, 316–328 (2009).
692 7. Schnöder, L. *et al.* Deficiency of Neuronal p38α MAPK Attenuates Amyloid
693 Pathology in Alzheimer Disease Mouse and Cell Models through Facilitating
694 Lysosomal Degradation of BACE1. *J. Biol. Chem.* **291**, 2067–2079 (2016).
695 8. Webber, J. L. & Tooze, S. A. New insights into the function of Atg9. *FEBS Lett.* **584**,
696 1319–1326 (2010).

697 9. Liu, B., Cheng, Y., Zhang, B., Bian, H. & Bao, J. Polygonatum cyrtonema lectin
698 induces apoptosis and autophagy in human melanoma A375 cells through a
699 mitochondria-mediated ROS-p38-p53 pathway. *Cancer Lett.* **275**, 54–60 (2009).
700 10. Younce, C. W. & Kolattukudy, P. E. MCP-1 causes cardiomyoblast death via
701 autophagy resulting from ER stress caused by oxidative stress generated by
702 inducing a novel zinc-finger protein, MCPIP. *Biochem. J.* **426**, 43–53 (2010).
703 11. Duan, W.-J. *et al.* Silibinin activated p53 and induced autophagic death in human
704 fibrosarcoma HT1080 cells via reactive oxygen species-p38 and c-Jun N-terminal
705 kinase pathways. *Biol. Pharm. Bull.* **34**, 47–53 (2011).
706 12. Zhuang, Y., Li, Y., Li, X., Xie, Q. & Wu, M. Atg7 Knockdown Augments Concanavalin
707 A-Induced Acute Hepatitis through an ROS-Mediated p38/MAPK Pathway. *PloS One*
708 **11**, e0149754 (2016).
709 13. Henson, S. M. *et al.* p38 signaling inhibits mTORC1-independent autophagy in
710 senescent human $CD8^+$ T cells. *J. Clin. Invest.* **124**, 4004–4016 (2014).
711 14. Luo, Y. *et al.* Autophagy regulates ROS-induced cellular senescence via p21 in a
712 p38 MAPKα dependent manner. *Exp. Gerontol.* **46**, 860–867 (2011).
713 15. Rudolf, E., Rezáčová, K. & Cervinka, M. Activation of p38 and changes in
714 mitochondria accompany autophagy to premature senescence-like phenotype switch
715 upon chronic exposure to selenite in colon fibroblasts. *Toxicol. Lett.* **231**, 29–37
716 (2014).
717 16. Vrailas-Mortimer, A. *et al.* A muscle-specific p38 MAPK/Mef2/MnSOD pathway
718 regulates stress, motor function, and life span in Drosophila. *Dev. Cell* **21**, 783–795
719 (2011).
720 17. Belozerov, V. E., Ratkovic, S., McNeill, H., Hilliker, A. J. & McDermott, J. C. In vivo
721 interaction proteomics reveal a novel p38 mitogen-activated protein kinase/Rack1

722 pathway regulating proteostasis in Drosophila muscle. *Mol. Cell. Biol.* **34**, 474–484
723 (2014).
724 18. Guruharsha, K. G. *et al.* A protein complex network of Drosophila melanogaster. *Cell*
725 **147**, 690–703 (2011).
726 19. Arndt, V. *et al.* Chaperone-assisted selective autophagy is essential for muscle
727 maintenance. *Curr. Biol. CB* **20**, 143–148 (2010).
728 20. Stürner, E. & Behl, C. The Role of the Multifunctional BAG3 Protein in Cellular
729 Protein Quality Control and in Disease. *Front. Mol. Neurosci.* **10**, 177 (2017).
730 21. Behl, C. BAG3 and friends: co-chaperones in selective autophagy during aging and
731 disease. *Autophagy* **7**, 795–798 (2011).
732 22. Gamerdinger, M. *et al.* Protein quality control during aging involves recruitment of
733 the macroautophagy pathway by BAG3. *EMBO J.* **28**, 889–901 (2009).
734 23. Kettern, N., Dreiseidler, M., Tawo, R. & Höhfeld, J. Chaperone-assisted degradation:
735 multiple paths to destruction. *Biol. Chem.* **391**, 481–489 (2010).
736 24. Min, J.-N. *et al.* CHIP deficiency decreases longevity, with accelerated aging
737 phenotypes accompanied by altered protein quality control. *Mol. Cell. Biol.* **28**, 4018–
738 4025 (2008).
739 25. Terman, A., Gustafsson, B. & Brunk, U. T. Autophagy, organelles and ageing. *J.*
740 *Pathol.* **211**, 134–143 (2007).
741 26. Dietzl, G. *et al.* A genome-wide transgenic RNAi library for conditional gene
742 inactivation in Drosophila. *Nature* **448**, 151–156 (2007).
743 27. R. C. Team. R Foundation for Statistical Computing. (2015).
744 28. Lim, K. L. *et al.* Parkin mediates nonclassical, proteasomal-independent
745 ubiquitination of synphilin-1: implications for Lewy body formation. *J. Neurosci. Off.*
746 *J. Soc. Neurosci.* **25**, 2002–2009 (2005).

747 29. Olzmann, J. A. *et al.* Parkin-mediated K63-linked polyubiquitination targets misfolded
748 DJ-1 to aggresomes via binding to HDAC6. *J. Cell Biol.* **178**, 1025–1038 (2007).
749 30. Yung, C., Sha, D., Li, L. & Chin, L.-S. Parkin Protects Against Misfolded SOD1
750 Toxicity by Promoting Its Aggresome Formation and Autophagic Clearance. *Mol.*
751 *Neurobiol.* **53**, 6270–6287 (2016).
752 31. Hao, R. *et al.* Proteasomes activate aggresome disassembly and clearance by
753 producing unanchored ubiquitin chains. *Mol. Cell* **51**, 819–828 (2013).
754 32. Tan, J. M. M. *et al.* Lysine 63-linked ubiquitination promotes the formation and
755 autophagic clearance of protein inclusions associated with neurodegenerative
756 diseases. *Hum. Mol. Genet.* **17**, 431–439 (2008).
757 33. Katsuragi, Y., Ichimura, Y. & Komatsu, M. p62/SQSTM1 functions as a signaling hub
758 and an autophagy adaptor. *FEBS J.* **282**, 4672–4678 (2015).
759 34. Ulbricht, A. *et al.* Cellular mechanotransduction relies on tension-induced and
760 chaperone-assisted autophagy. *Curr. Biol. CB* **23**, 430–435 (2013).
761 35. Hattori, A., Mizuno, T., Akamatsu, M., Hisamoto, N. & Matsumoto, K. The
762 Caenorhabditis elegans JNK Signaling Pathway Activates Expression of Stress
763 Response Genes by Derepressing the Fos/HDAC Repressor Complex. *PLOS*
764 *Genet.* **9**, e1003315 (2013).
765 36. Coulson, M., Robert, S. & Saint, R. Drosophila starvin encodes a tissue-specific
766 BAG-domain protein required for larval food uptake. *Genetics* **171**, 1799–1812
767 (2005).
768 37. Sato, T. *et al.* DNAJB6 myopathy in an Asian cohort and cytoplasmic/nuclear
769 inclusions. *Neuromuscul. Disord. NMD* **23**, 269–276 (2013).
770 38. Selcen, D. *et al.* Mutation in BAG3 causes severe dominant childhood muscular
771 dystrophy. *Ann. Neurol.* **65**, 83–89 (2009).

772 39. Sarparanta, J. *et al.* Mutations affecting the cytoplasmic functions of the co-
773 chaperone DNAJB6 cause limb-girdle muscular dystrophy. *Nat. Genet.* **44**, 450–455,
774 S1-2 (2012).
775 40. Fanzani, A. *et al.* Hypertrophy and atrophy inversely regulate Caveolin-3 expression
776 in myoblasts. *Biochem. Biophys. Res. Commun.* **357**, 314–318 (2007).
777 41. Capanni, C. *et al.* Dysferlin in a hyperCKaemic patient with caveolin 3 mutation and
778 in C2C12 cells after p38 MAP kinase inhibition. *Exp. Mol. Med.* **35**, 538–544 (2003).
779 42. Suzuki, N. *et al.* Continuous administration of poloxamer 188 reduces overload-
780 induced muscular atrophy in dysferlin-deficient SJL mice. *Neurosci. Res.* **72**, 181–
781 186 (2012).
782 43. De Sandre-Giovannoli, A. *et al.* Lamin a truncation in Hutchinson-Gilford progeria.
783 *Science* **300**, 2055 (2003).
784 44. Eriksson, M. *et al.* Recurrent de novo point mutations in lamin A cause Hutchinson-
785 Gilford progeria syndrome. *Nature* **423**, 293–298 (2003).
786 45. Mounkes, L. C., Kozlov, S., Hernandez, L., Sullivan, T. & Stewart, C. L. A progeroid
787 syndrome in mice is caused by defects in A-type lamins. *Nature* **423**, 298–301
788 (2003).
789 46. Singla, A. *et al.* Lamin aggregation is an early sensor of porphyria-induced liver
790 injury. *J. Cell Sci.* **126**, 3105–3112 (2013).
791 47. Bank, E. M. *et al.* A laminopathic mutation disrupting lamin filament assembly
792 causes disease-like phenotypes in Caenorhabditis elegans. *Mol. Biol. Cell* **22**, 2716–
793 2728 (2011).
794 48. Casasola, A. *et al.* Prelamin A processing, accumulation and distribution in normal
795 cells and laminopathy disorders. *Nucleus* **7**, 84–102 (2016).
796 49. Dialynas, G. *et al.* Myopathic Lamin Mutations Cause Reductive Stress and Activate
797 the Nrf2/Keap-1 Pathway. *PLOS Genet.* **11**, e1005231 (2015).

798 50. Hübner, S., Eam, J. E., Hübner, A. & Jans, D. A. Laminopathy-inducing lamin A
799 mutants can induce redistribution of lamin binding proteins into nuclear aggregates.
800 *Exp. Cell Res.* **312**, 171–183 (2006).
801 51. Hübner, S., Eam, J. E., Wagstaff, K. M. & Jans, D. A. Quantitative analysis of
802 localization and nuclear aggregate formation induced by GFP-lamin A mutant
803 proteins in living HeLa cells. *J. Cell. Biochem.* **98**, 810–826 (2006).
804 52. Ahmed, M. S., Ikram, S., Bibi, N. & Mir, A. Hutchinson-Gilford Progeria Syndrome: A
805 Premature Aging Disease. *Mol. Neurobiol.* **55**, 4417–4427 (2018).
806 53. Barascu, A. *et al.* Oxidative stress induces an ATM-independent senescence
807 pathway through p38 MAPK-mediated lamin B1 accumulation. *EMBO J.* **31**, 1080–
808 1094 (2012).
809 54. Zaremba-Czogalla, M. *et al.* The Different Function of Single Phosphorylation Sites
810 of Drosophila melanogaster Lamin Dm and Lamin C. *PLoS ONE* **7**, (2012).
811 55. Li, Y. *et al.* Lamin Mutations Accelerate Aging via Defective Export of Mitochondrial
812 mRNAs through Nuclear Envelope Budding. *Curr. Biol. CB* **26**, 2052–2059 (2016).
813 56. Muñoz-Alarcón, A. *et al.* Characterization of lamin Mutation Phenotypes in
814 Drosophila and Comparison to Human Laminopathies. *PLOS ONE* **2**, e532 (2007).
815 57. Kitten, G. T. & Nigg, E. A. The CaaX motif is required for isoprenylation, carboxyl
816 methylation, and nuclear membrane association of lamin B2. *J. Cell Biol.* **113**, 13–23
817 (1991).
818 58. Holtz, D., Tanaka, R. A., Hartwig, J. & McKeon, F. The CaaX motif of lamin A
819 functions in conjunction with the nuclear localization signal to target assembly to the
820 nuclear envelope. *Cell* **59**, 969–977 (1989).
821 59. Meshorer, E. & Gruenbaum, Y. Gone with the Wnt/Notch: stem cells in
822 laminopathies, progeria, and aging. *J. Cell Biol.* **181**, 9–13 (2008).

823 60. Polychronidou, M., Hellwig, A. & Grosshans, J. Farnesylated nuclear proteins
824 Kugelkern and lamin Dm0 affect nuclear morphology by directly interacting with the
825 nuclear membrane. *Mol. Biol. Cell* **21**, 3409–3420 (2010).
826 61. Patterson, K. *et al.* The functions of Klarsicht and nuclear lamin in developmentally
827 regulated nuclear migrations of photoreceptor cells in the Drosophila eye. *Mol. Biol.*
828 *Cell* **15**, 600–610 (2004).
829 62. Cao, K., Capell, B. C., Erdos, M. R., Djabali, K. & Collins, F. S. A lamin A protein
830 isoform overexpressed in Hutchinson-Gilford progeria syndrome interferes with
831 mitosis in progeria and normal cells. *Proc. Natl. Acad. Sci. U. S. A.* **104**, 4949–4954
832 (2007).
833 63. Machowska, M., Piekarowicz, K. & Rzepecki, R. Regulation of lamin properties and
834 functions: does phosphorylation do it all? *Open Biol.* **5**, (2015).
835 64. Saito, A., Kawai, K., Takayama, H., Sudo, T. & Osada, H. Improvement of
836 photoaffinity SPR imaging platform and determination of the binding site of
837 p62/SQSTM1 to p38 MAP kinase. *Chem. Asian J.* **3**, 1607–1612 (2008).
838 65. Rana, A., Rera, M. & Walker, D. W. Parkin overexpression during aging reduces
839 proteotoxicity, alters mitochondrial dynamics, and extends lifespan. *Proc. Natl. Acad.*
840 *Sci. U. S. A.* **110**, 8638–8643 (2013).
841 66. Burke, B. & Stewart, C. L. The nuclear lamins: flexibility in function. *Nat. Rev. Mol.*
842 *Cell Biol.* **14**, 13–24 (2013).
843

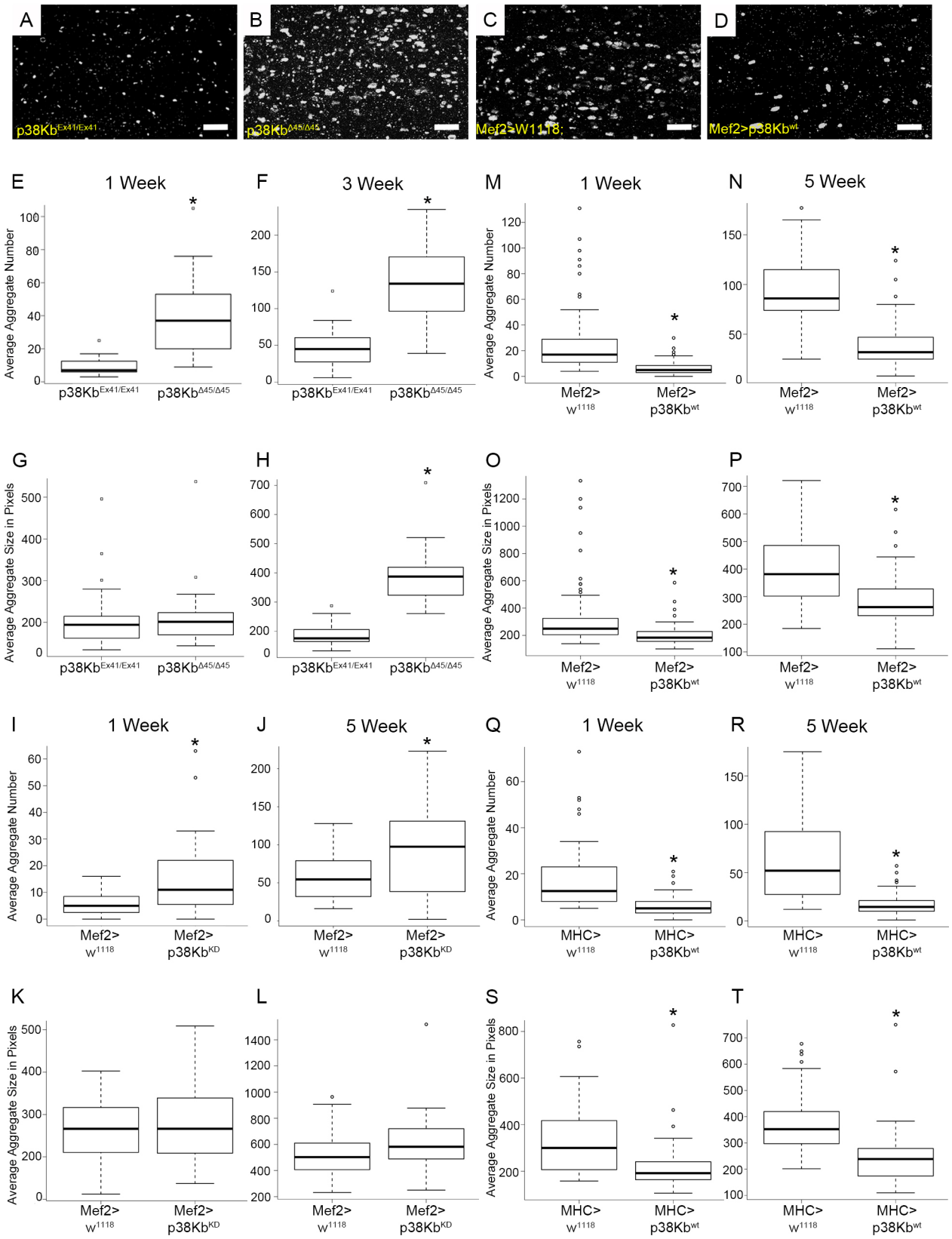
A
B
C
D
p38Kb$^{Ex41/Ex41}$
p38Kb$^{\Delta45/\Delta45}$
Mef2>W1118
Mef2>p38Kb^{wt}
E
1 Week
F
3 Week
M
1 Week
N
5 Week
Average Aggregate Number
p38Kb$^{Ex41/Ex41}$
p38Kb$^{\Delta45/\Delta45}$
Mef2> w^{1118}
Mef2> p38Kb^{wt}
G
H
O
P
Average Aggregate Size in Pixels
I
1 Week
J
5 Week
Q
1 Week
R
5 Week
Mef2> w^{1118}
Mef2> p38Kb^{KD}
MHC> w^{1118}
MHC> p38Kb^{wt}
K
L
S
T

Figure 1

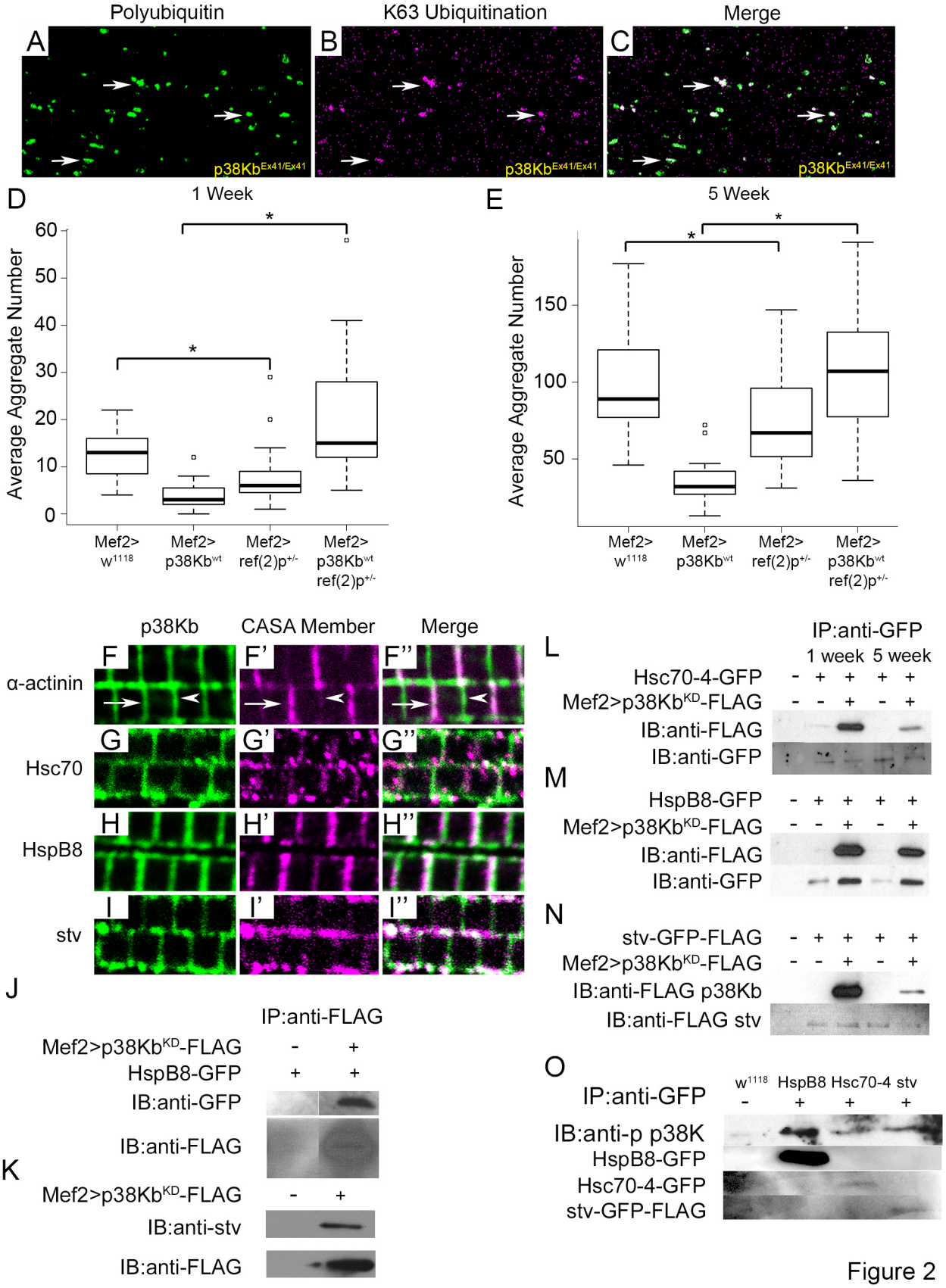
Polyubiquitin
K63 Ubiquitination
Merge
A
B
C
p38Kb^Ex41/Ex41
D
1 Week
Average Aggregate Number
Mef2> w^1118
Mef2> p38Kb^wt
Mef2> ref(2)p^+/-
Mef2> p38Kb^wt ref(2)p^+/-
E
5 Week
p38Kb
CASA Member
Merge
α-actinin
Hsc70
HspB8
stv
F
F'
F''
G
G'
G''
H
H'
H''
I
I'
I''
J
IP:anti-FLAG
Mef2>p38Kb^KD-FLAG
HspB8-GFP
IB:anti-GFP
IB:anti-FLAG
K
IB:anti-stv
L
IP:anti-GFP
1 week 5 week
Hsc70-4-GFP
IB:anti-FLAG
IB:anti-GFP
M
HspB8-GFP
N
stv-GFP-FLAG
IB:anti-FLAG p38Kb
IB:anti-FLAG stv
O
w^1118 HspB8 Hsc70-4 stv
IB:anti-p p38K
HspB8-GFP
Hsc70-4-GFP
stv-GFP-FLAG

Figure 2

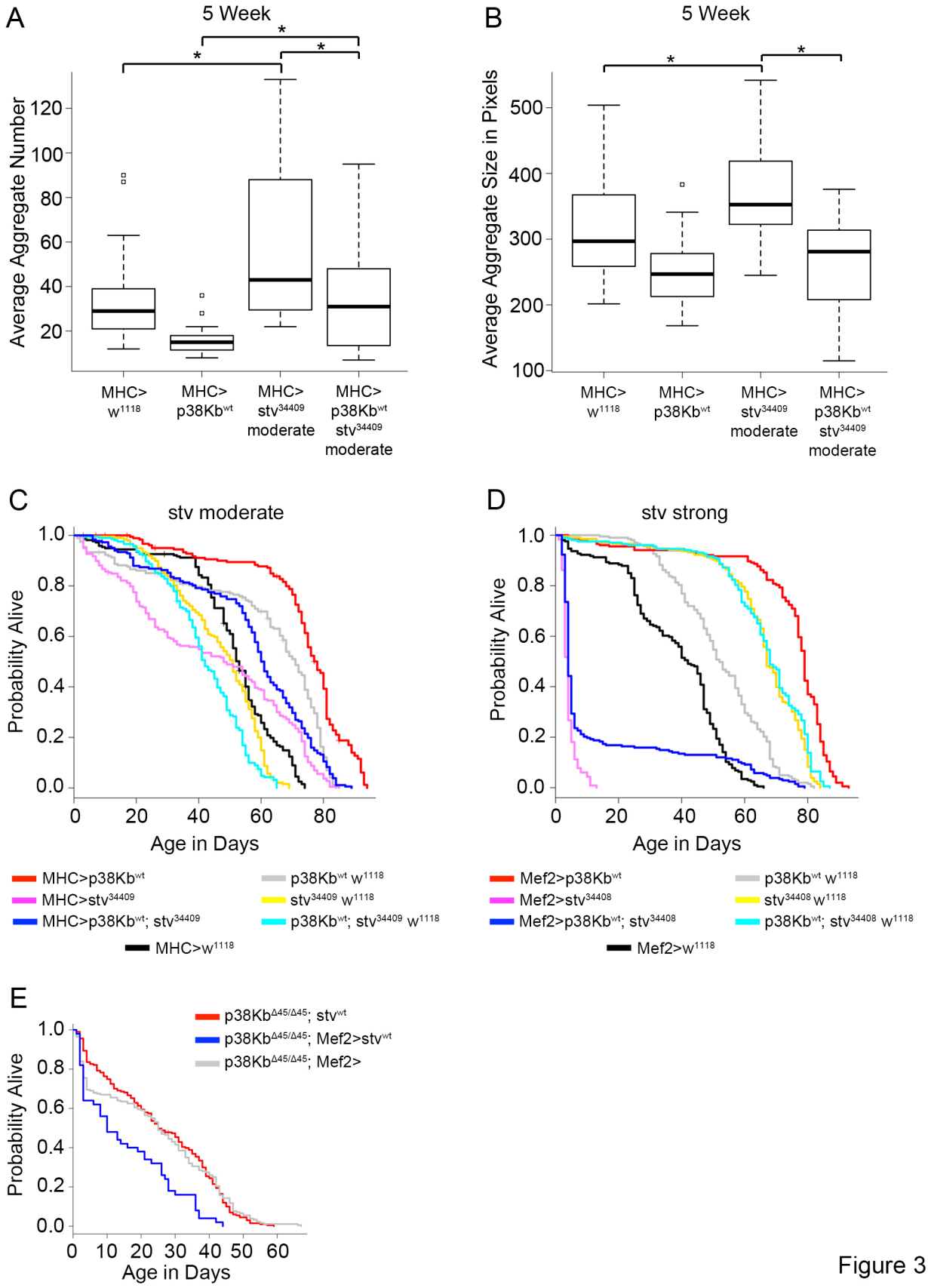
A
5 Week
Average Aggregate Number
MHC> w1118
MHC> p38Kbwt
MHC> stv34409 moderate
MHC> p38Kbwt stv34409 moderate
B
5 Week
Average Aggregate Size in Pixels
C
stv moderate
Probability Alive
Age in Days
MHC>p38Kbwt
MHC>stv34409
MHC>p38Kbwt; stv34409
MHC>w1118
p38Kbwt w1118
stv34409 w1118
p38Kbwt; stv34409 w1118
D
stv strong
Mef2>p38Kbwt
Mef2>stv34408
Mef2>p38Kbwt; stv34408
Mef2>w1118
p38Kbwt w1118
stv34408 w1118
p38Kbwt; stv34408 w1118
E
p38KbΔ45/Δ45; stvwt
p38KbΔ45/Δ45; Mef2>stvwt
p38KbΔ45/Δ45; Mef2>

Figure 3

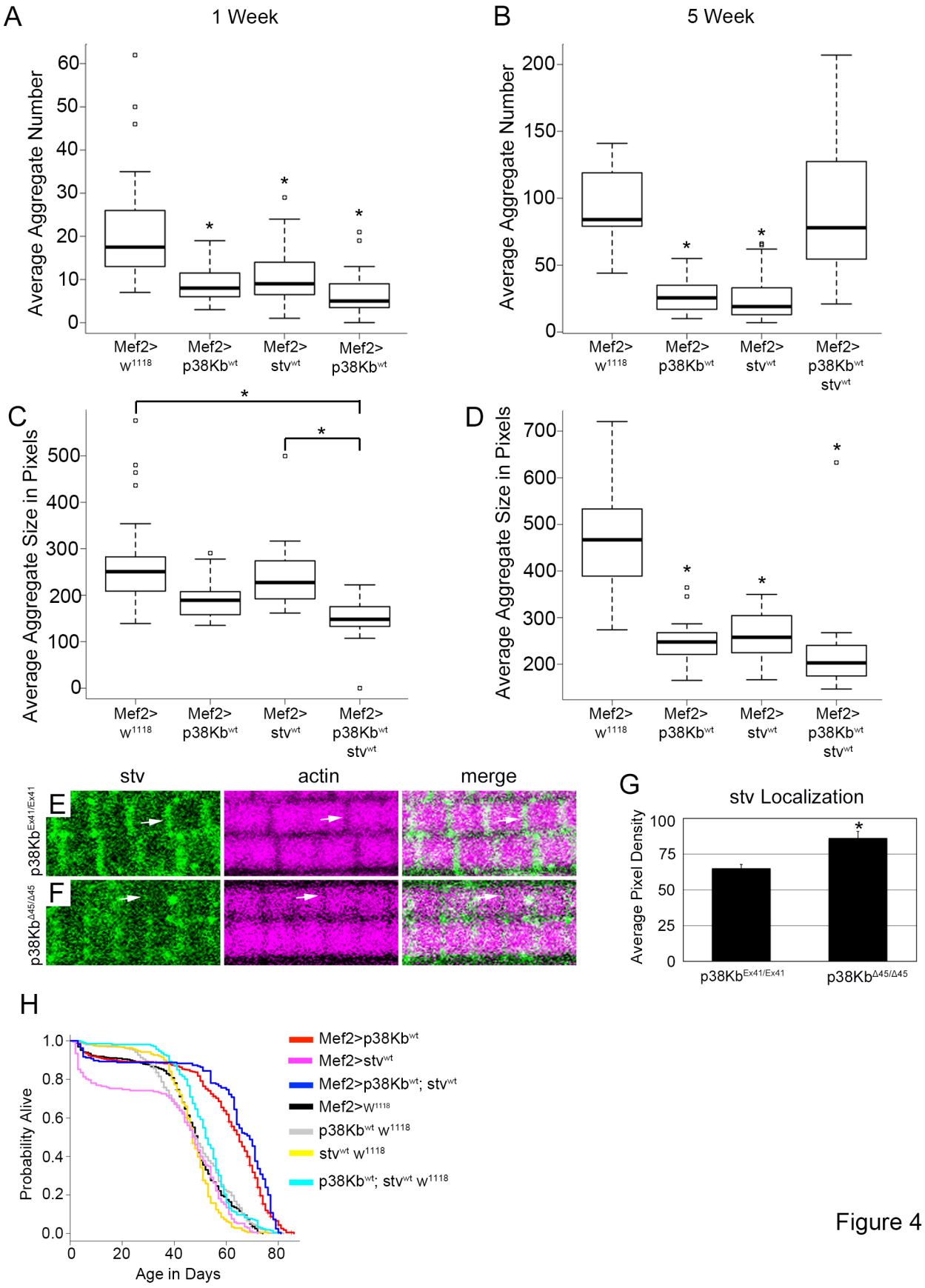
A
1 Week
Average Aggregate Number
Mef2> w1118
Mef2> p38Kbwt
Mef2> stvwt
Mef2> p38Kbwt
B
5 Week
Average Aggregate Number
Mef2> w1118
Mef2> p38Kbwt
Mef2> stvwt
Mef2> p38Kbwt stvwt
C
Average Aggregate Size in Pixels
Mef2> w1118
Mef2> p38Kbwt
Mef2> stvwt
Mef2> p38Kbwt stvwt
D
Average Aggregate Size in Pixels
Mef2> w1118
Mef2> p38Kbwt
Mef2> stvwt
Mef2> p38Kbwt stvwt
stv
actin
merge
E
p38KbEx41/Ex41
F
p38KbΔ45/Δ45
G
stv Localization
Average Pixel Density
p38KbEx41/Ex41
p38KbΔ45/Δ45
H
Probability Alive
Age in Days
Mef2>p38Kbwt
Mef2>stvwt
Mef2>p38Kbwt; stvwt
Mef2>w1118
p38Kbwt w1118
stvwt w1118
p38Kbwt; stvwt w1118

Figure 4

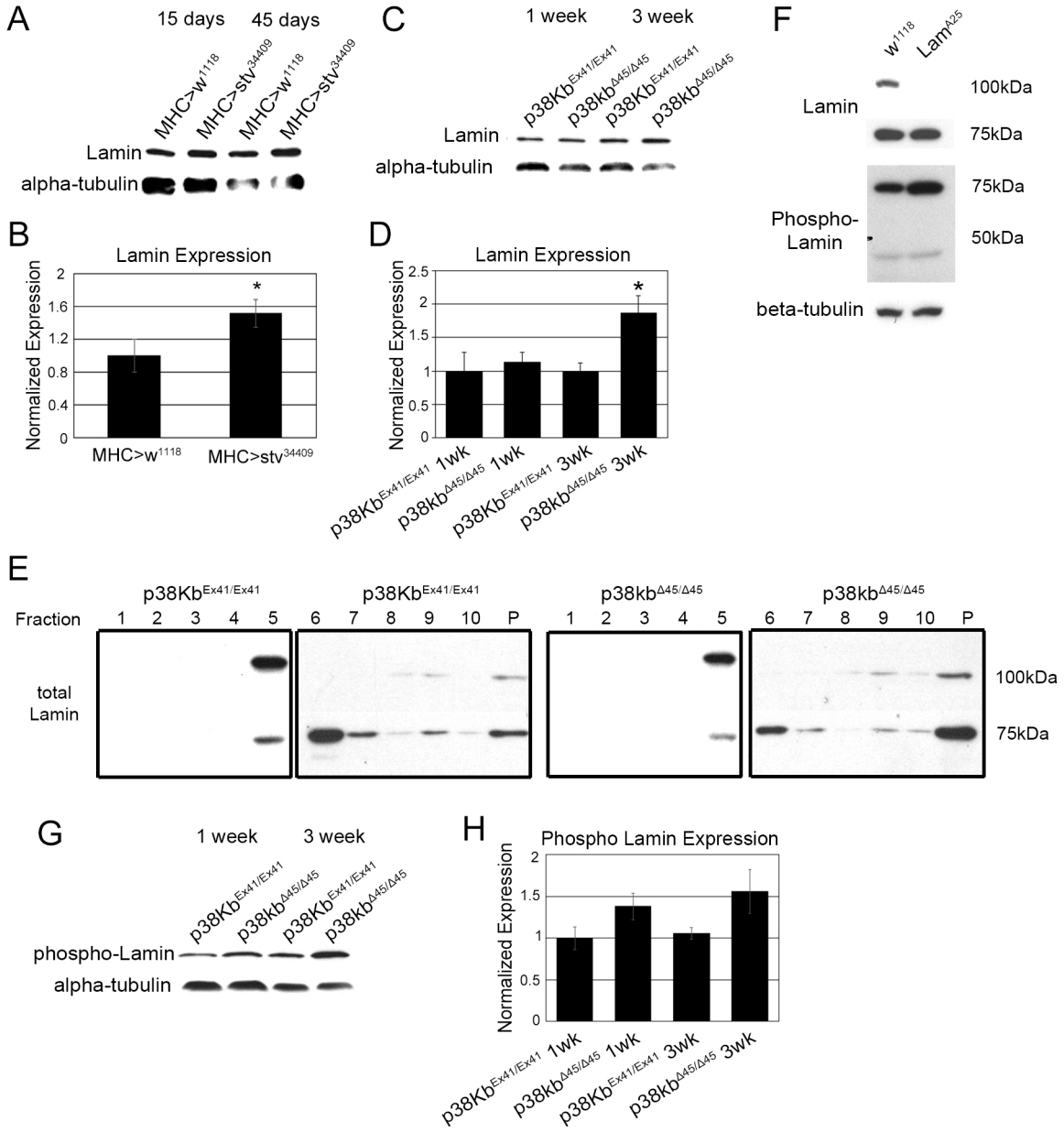
A
15 days
45 days
MHC>w1118
MHC>stv34409
MHC>w1118
MHC>stv34409
Lamin
alpha-tubulin
B
Lamin Expression
Normalized Expression
MHC>w1118
MHC>stv34409
C
1 week
3 week
p38KbEx41/Ex41
p38kbΔ45/Δ45
p38KbEx41/Ex41
p38kbΔ45/Δ45
Lamin
alpha-tubulin
D
Lamin Expression
Normalized Expression
p38KbEx41/Ex41 1wk
p38kbΔ45/Δ45 1wk
p38KbEx41/Ex41 3wk
p38kbΔ45/Δ45 3wk
F
w1118
LamA25
Lamin
100kDa
75kDa
75kDa
Phospho-Lamin
50kDa
beta-tubulin
E
p38KbEx41/Ex41
p38KbEx41/Ex41
p38kbΔ45/Δ45
p38kbΔ45/Δ45
Fraction
1 2 3 4 5 6 7 8 9 10 P
total Lamin
100kDa
75kDa
G
1 week
3 week
p38KbEx41/Ex41
p38kbΔ45/Δ45
p38KbEx41/Ex41
p38kbΔ45/Δ45
phospho-Lamin
alpha-tubulin
H
Phospho Lamin Expression
Normalized Expression
p38KbEx41/Ex41 1wk
p38kbΔ45/Δ45 1wk
p38KbEx41/Ex41 3wk
p38kbΔ45/Δ45 3wk
I
p38KbEx41/Ex41
p38KbEx41/Ex41
p38kbΔ45/Δ45
p38kbΔ45/Δ45
Fraction
1 2 3 4 5 6 7 8 9 10 P
phospho Lamin
75kDa
50kDa

Figure 5

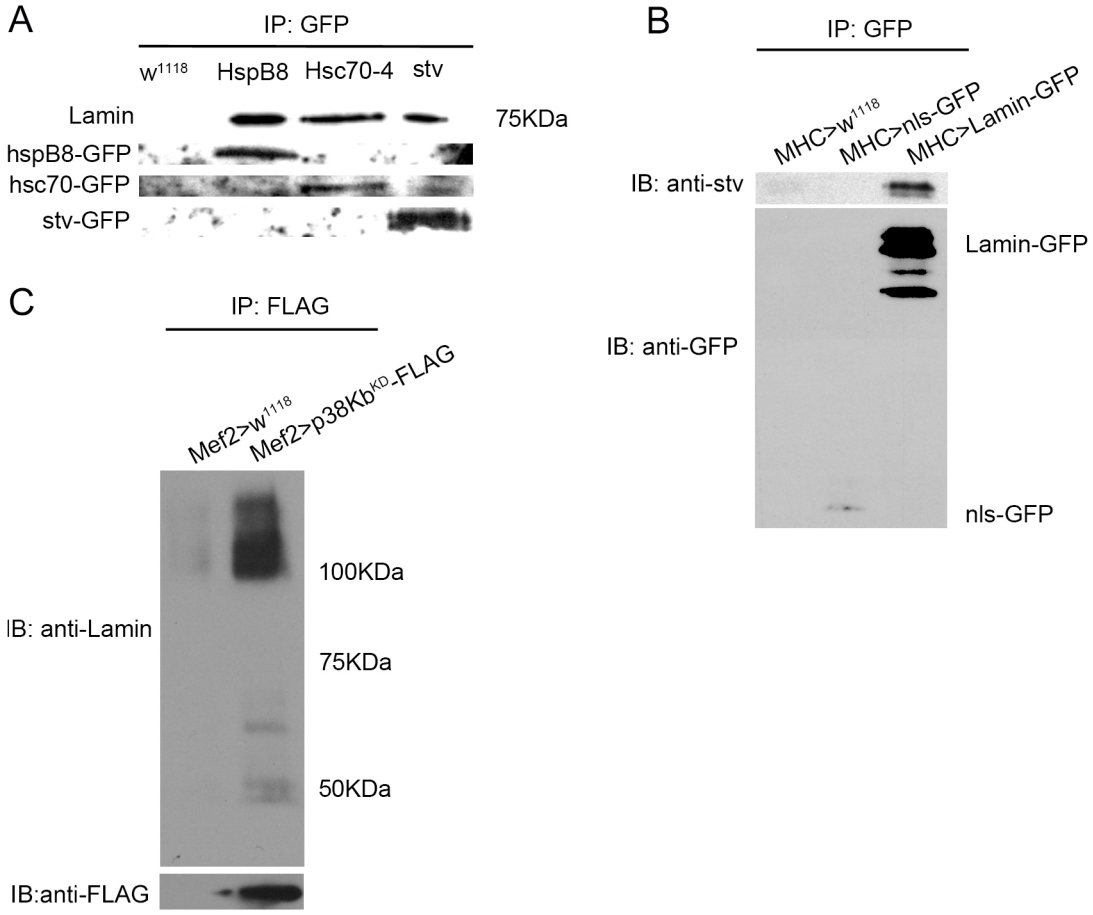
A
IP: GFP
w1118
HspB8
Hsc70-4
stv
Lamin
75KDa
hspB8-GFP
hsc70-GFP
stv-GFP
B
IP: GFP
MHC>w1118
MHC>nls-GFP
MHC>Lamin-GFP
IB: anti-stv
Lamin-GFP
IB: anti-GFP
nls-GFP
C
IP: FLAG
Mef2>w1118
Mef2>p38KbKD-FLAG
100KDa
IB: anti-Lamin
75KDa
50KDa
IB:anti-FLAG

Figure 6